Energy balance in dense microemulsions

Journal of Thermal Analysis and Calorimetry, Vol. 92 (2008) 2, 535–541

ENERGY BALANCE IN DENSE MICROEMULSIONS

Donatella Senatra[1,2], *C. Ziparo*[2,3], *Cecilia M. C. Gambi*[1,2*] *and L. Lanzi*[1]

[1]Department of Physics and CNISM University of Florence, via Sansone 1, 50019 Sesto Fiorentino, Florence, Italy
[2]CRS-Soft Matter (CNR-INFM) Università di Roma 'La Sapienza', p.le A. Moro 2, 00185 Roma, Italy
[3]European Laboratory for Non-linear Spectroscopy (LENS), via Carrara 1, 50019 Sesto Fiorentino, Florence, Italy

A water-in-oil microemulsion composed of water, AOT and decane with volume fraction ϕ=0.50 and molar ratio X=40.8 was analysed by DSC. The percolation and the bicontinuous transitions as well as the melting endotherms and the freezing exotherms were measured. The main attention was focussed on the system energy balance. It was found that, by freezing the samples after the occurrence of the percolative transition, the total heat released is significantly less than the heat absorbed in the melting endotherms. A simple geometrical model was used as an analysis tool of the aforementioned energy difference. Since the system studied exhibits a percolative transition of dynamic type, on approaching the percolation threshold temperature ($T \leq T_p$) and a static percolation for $T \geq T_p$, the structural change from the connecting water-droplet-cluster to a connecting water channel was schematised in the model as a change from a sphere-necklace to a water-cylindrical channel of equal volume and equal length. The surface energy associated with the formation of the two different geometrical surfaces was evaluated and the amount of saved energy compared with the experimentally measured one.

Keywords: *dense microemulsions, energy balance, percolation and bicontinuous transitions by DSC*

Introduction

The present paper deals with the results obtained by thermal analysis on a water-in-oil microemulsion composed of water, AOT and decane [1]. The AOT (sodium di-2-ethyl hexyl sulphosuccinate) is a surfactant with two bulky hydrocarbon chains and a small ionic head group. This surfactant is poorely soluble in water but highly soluble in the decane oil. It forms reverse micelles that, upon water addition, can solubilize a notable amount of water which is incorporated into the hydrophilic micellar core, giving rise to swollen inverted micelles dispersed in a continuous decane phase.

The parameters that characterize the composition of this three-component system are the volume fraction Φ=Vol·(H_2O+AOT)/total volume and the molar ratio X=[H_2O]/[AOT]. The latter is the number of water molecules incorporated into the swollen micelle per surfactant molecule. For any given X the mean radius of the droplets is fixed. The droplet size depends linearly on the water/AOT molar ratio [2, 3].

The system investigated has Φ=0.50 and X=40.8; for this composition, the condition of not interacting droplets [4] fails to apply and the water-in-oil dispersion is identified as 'dense microemulsion' [2]. The system exhibits the percolation phenomenon and, by rising the temperature above the percolation threshold temperature, forms bicontinuous structures [5].

In this study both the percolative behavior and the bicontinuous structural assessment are investigated by differential scanning calorimetry (DSC) [6, 7]. The leading parameters are: the temperature and the thermal program followed.

The attention is focussed on: 1) The energy balance between the heat adsorbed in the melting endotherms and that released in the freezing exotherms; 2) The energy associated with the formation of the internal surface (surface energy); 3) The energy difference corresponding to the structural change from a droplet-necklace, immediately before the percolative threshold temperature (T_p), to the water-channel that forms at a temperature immediately after T_p.

As an analysis tool, an extremely simple geometrical model was utilized to help evidencing the energetics of the structural change from the necklace of water spheres to a water channel of equal length, with the aim to obtain an estimate of the order of magnitude of the energy 'saved' in this process. The estimated energy was thereafter compared with the experimental results.

Experimental

Materials and methods

Composition of the microemulsion system

The system is composed of water (Millipore Milli-Q-System quality), Decane (Sigma +99% purity) and AOT (Fluka 99% purity) purified again

* Author for correspondence: gambi@fi.infn.it

1388–6150/$20.00

Akadémiai Kiadó, Budapest, Hungary
Springer, Dordrecht, The Netherlands

according to the procedure reported in [8]. The microemulsion has ϕ=0.50 and X=40.8.

During the research the above system was prepared three times in small amounts from which the samples were taken. The above procedure was followed in order to have always good, reliable samples and to avoid the AOT hydrolysis [9]. Since it is impossible to formulate identical systems a small difference between the proportions of the components has resulted. The three compositions are reported in Table 1.

DSC analysis

The thermal analysis was performed with a Mettler-Toledo TA 4000 Differential Scanning Calorimeter equipped with a low temperature silver cell model DSC S-30. The measuring range in the actual configuration was 50 mW. The temperature interval investigated extends from 343 down to 173 K. Thermal rates from 1 to 10 K min^{-1} were used. The samples were sealed into aluminum pans. Sample masses ranging between 2 and 8 mg were employed. The sample mass was measured with an accuracy of ±2 μg with a Mettler-Toledo balance Model MX5. After each measuring run, the mass of the aluminum pan filled with the sample was checked in order to exclude any leakage during the measure. Nitrogen gas of 5.5 purity was used to purge the cell. During the DSC analysis of the percolation and the bicontinuous transitions no purging gas was used while a flow of 20 mL min^{-1} was employed in the melting and freezing DSC spectra study. In order to simplify the measuring procedure, two aluminum pans of equal mass were used for both the reference and the sample holder pans. The temperature program imposed to the samples was the following: the samples were taken isothermally for 30 min at 290 K and thereafter, from the latter temperature, to 293 K with 1 K min^{-1} thermal rate. In order to trigger the percolative transition, a ΔT change was realized by lowering the sample temperature to 258 K [10, 11]. Then, for the measure of the percolative behavior, the temperature was rised with a 10 K min^{-1} rate to 313 K, and to 333 K for the DSC analysis of the bicontinuous transition. We point out that the freezing exotherms have confirmed that at 258 K the water component of the sample is not frozen because of the overcooling phenomenon [12].

A reversibility test was performed for both the percolation and the bicontinuous transitions in the temperature range of 313–258 and 333–258 K, respectively.

The freezing exotherms were measured with a 2 K min^{-1} rate, in the T-ranges 290–183 and 333–183 K, the melting endotherms with the same thermal rate in the T-ranges 183–290 and 183–333 K.

The measured parameter in the DSC analysis is the heat absorbed in the endothermic process or that released in the exothermic one. The enthalpy change ΔH (J g^{-1} of sample) associated with the melting (and/or) the freezing of each one of the two liquid components of the microemulsion sample was evaluated.

The melting spectra, obtained upon melting the previously frozen microemulsion, show two thermal events that can be identified on the basis of the temperatures at which their melting occurs. Previous work [6, 12] has demonstrated that both the dispersed water phase and the dispersing oil phase behave as massive bulk phases, as indicated by their melting at the melting temperature of the corresponding pure liquids (Fig. 1).

The enthalpy values associated with the water and the oil thermal events are the experimentally measured data, labelled ΔH_w and ΔH_d expressed in J g^{-1} of sample. However, if one calculates the a priori expected enthalpy value ($\Delta H°_w$) for example due to the melting of the known amount of water contained in the sample, it is possible to realize that not all the water of the sample melts because $\Delta H°_w >> \Delta H_w$.

The fraction of water that behaves as free (melting at 273 K) can be estimated as well as the amount of water that being not free, it is not directly evident in the DSC spectra. The procedure for the calculation of the different enthalpic contributions as well as other information, e.g. pertaining the surfactant is reported in [6, 10].

Since freezing and melting processes are first order phase transitions they must be reversible and thermal-rate independent. This is confirmed in the DSC study of microemulsions. However, due to the overcooling phenomenon, the two liquid phases water and oil freeze at a much lower temperature than 273 and 243.3 K (Fig. 1). We recall that the percolative nature of the microemulsion was found to emerge directly from the exotherms associated with the freezing of the water phase. The latter topic,

Table 1 Composition of the three microemulsion system, a, b and c

Component	Symbol	a/mg	%	b/mg	%	c/mg	%	Φ	X
Decane	O	715.2	41.12	698.6	40.84	717.4	41.05	0.4999[a]	40.796[a]
AOT	S	385.9	22.20	381.4	22.30	388.0	22.20	0.5028[b]	40.78[b]
Water	W	638.0	36.68	630.4	36.86	642.2	36.75	0.5007[c]	40.842[c]
Total mass		1739.1		1710.4		1747.6			

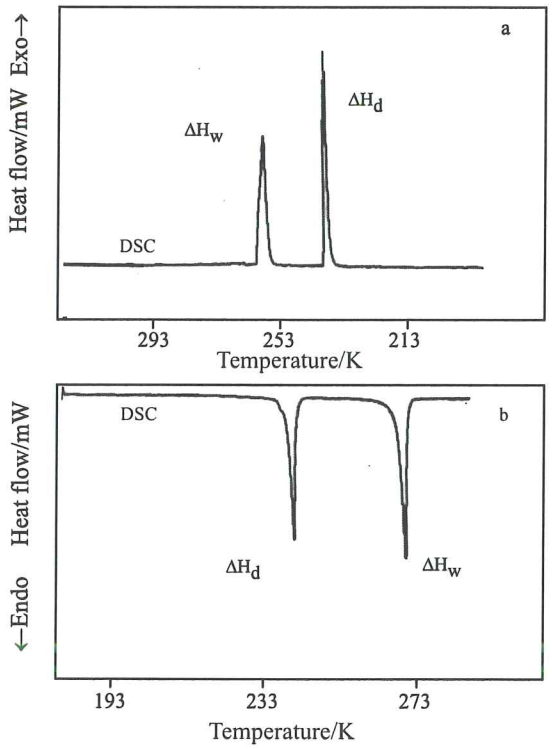

Fig. 1 a – Freezing exotherms and b – melting endotherms of a sample in the microemulsion state. In curve (a) note the overcooling of the two liquid components water and decane. Sample-composition (b) of Table 1

described in detail in previous works [11, 12] will not be discussed in the present paper. The calorimetric reference data are reported in Table 2.

The geometric model

The geometric model is valid only for the case of the percolation transition exhibited by the actual system investigated. Rouch [5] found that for $T \leq T_p$, immediately before the percolative threshold temperature T_p at which the very first connecting cluster of droplets forms, the mechanism of percolation is of dynamic type; this means that the droplets do not loose their droplet-identity, while at $T \geq T_p$ the mechanism of percolation is static; the droplets coalesce and form a connecting water channel.

The process is sketched in Fig. 2-top. If we eliminate the AOT surfactant from the droplet-

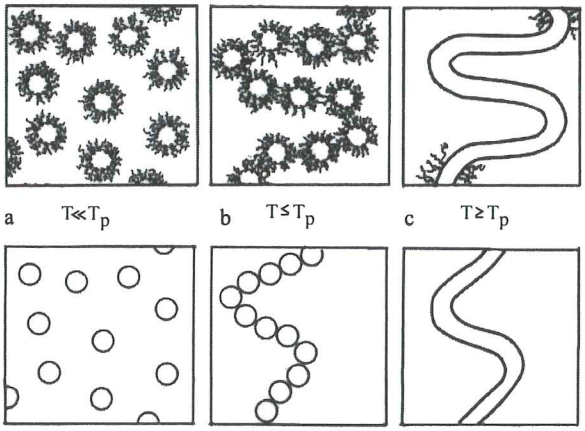

Fig. 2 Top – a – schematic representation of the *w/o* microemulsion. The reverse AOT micelles in the decane oil are omitted. b – the formation of the water-droplet cluster at $T \leq T_P$ (dynamic percolation); c – the formation of the connecting water channel at $T \geq T_P$. (static percolation). Bottom – the same situation drastically simplified for the model: only the droplet-cores are left. See text for farther explanation

interface, we obtain the situation featured in Fig. 2-bottom where only the water cores are left. The inverse AOT micelles in the decane oil are omitted.

The model attempts to evaluate how much surface energy is saved in the structural change from the droplet-connecting cluster to the equivalent water channel of equal length.

We assume that:

1 The cores of spherical shape initially distributed randomly for $T \ll T_p$ at $T \approx T_p$, form the first connecting droplet-cluster identified as the 'sphere-necklace'; correspondingly at $T \geq T_p$, the connecting water channel results from the coalescence of the same number of spheres composing the necklace. The channel has a cylindrical shape.
2 The 'surfaces' for both the spheres and the cylinder are geometrical surfaces.
3 Both the sphere-necklace and the connecting cylinder have the same length and contain the same volume of water; this water corresponds to the total available sample water content.
4 The density of water is exactly equal to 1 g cm^{-3}.
5 The elementary cylinder (V_C^1) corresponding to a single water sphere of the necklace (V_S^1) is consid-

Table 2 Calorimetric data

Component	T_m/K	T_{fz}/K	ΔH/J g^{-1}	MW
Water	273.0	253–233	333.13	18.016
Decane	243.3	233	202.00	142.28
AOT	–	–	–	446.54

T_m – melting temperature; T_{fz} – freezing temperature

Table 3 Values of the parameters used in the model

Single sphere	Elementary cylinder	Water molecule (w)
$R_S=50.00\cdot10^{-8}$ cm	$R_C=40.82\cdot10^{-8}$ cm	
$V_S=5.23\cdot10^{-19}$ cm^3	$V_C=5.23\cdot10^{-19}$ cm^3	$v_W=3.0\cdot10^{-23}$ cm^2 [13, 14]
$S_S=3.14\cdot10^{-12}$ cm^2	$S_C=2.56\cdot10^{-12}$ cm^2	$a_w=10.0\cdot10^{-16}$ cm^2 [13]
	$L_C=2\ R_S=100\cdot10^{-8}$ cm	–
		Surface tension=γ=72 mJ m^{-2}

a_w – Estimate of the area occupied by each water molecule at the surface

ered in order to evaluate its length (L) and its radius (R_c) with the condition $V_s=V_c$.

There are two possibilities:

i) we assume $L=2R_s$. Since $V^l{}_s=V^l{}_c$, the cylinder radius can be evaluated as $R_c=(V^l{}_s/\pi L)^{1/2}$

ii) we assume $R_c=R_s$ and evaluate $L=V^l{}_c/\pi R^2$

With option (*i*) the sphere equivalent-cylinder shrinks ($R_c<R_s$) but the sphere-necklace and the total water cylinder will be of the same length.

With option (*ii*) the radius is the same for both of them but the resulting length of the total cylinder will be less than that of the necklace.

Because of point 3 in the latter case there would be no more water left to complete the cylindrical channel and the connectedness of the sample would fail. Therefore, on the basis of the hypotheses formulated we must reject the (*ii*) option.

6 The purely geometrical model is linked to the real system only for what concerns the volume of the water in the sample and the mean value of the sphere radius R_s corresponding to the molar ratio X=40.8.

The values of the parameters used in the model are given in Table 3. The symbols and the estimated 'quantities' are reported in Table 4.

Results and discussion

Percolation and bicontinuous transitions

The direct recording of the percolation transition following the thermal program previously described, obtained on a sample taken from the 1st formulation of Table 1, is shown in Fig. 3a; the trend of the specific heat at constant pressure (C_P) as a function of increasing temperature, is plotted in Fig. 3b. The measure was stopped below the T-interval within which the bicontinuous structural change develops. The result of the reversibility test for the transition, in the same temperature range, but moving from the final (323 K) down to the starting temperature (258 K), is shown in Fig. 3c.

The direct measure of both the percolation and the bicontinuous transitions is plotted in Fig. 4a. The onset method has given for the two processes; T_p=292.6 K and T_B=322 K. In the latter case the trend

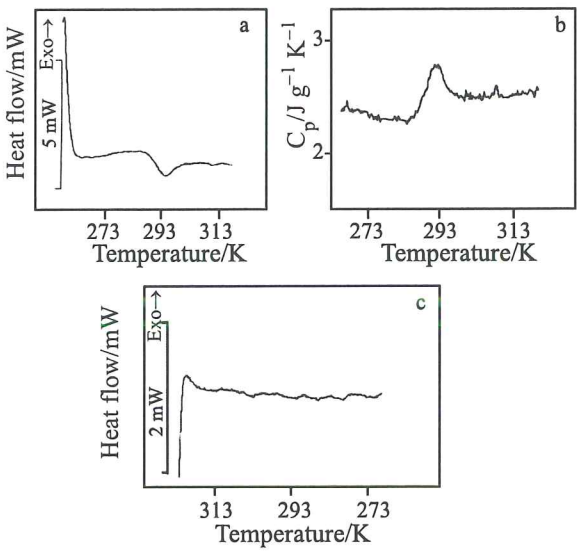

Fig. 3 a – percolation transition: direct recording. T_P=292.6 K. b – specific heat C_p as a function of temperature. c – reversibility test. Sample-composition (a) of Table 1

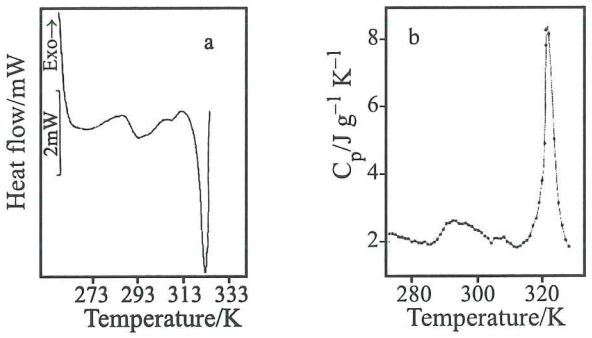

Fig. 4 a – the percolation and the bicontinuous transitions *vs.* increasing temperature. Direct recording. b – trend of the corresponding C_p upon rising the temperature. Sample composition (c) of Table 1

of the reversibility test in the range 333 – 258 K is the same as the one shown in Fig. 3c. The behavior of the specific heat C_P upon increasing temperature is reported in Fig. 4b.

As evidenced in previous papers [6, 10, 11] both processes exhibit a thermal hysteresis. The time–inter-

Table 4 Symbols used in the model

Total water volume V_T*	$^*V_T$
a – Sphere	
1 Total number of water spheres in the sample:	$N_S = V_T/V_S$
2 Number of water molecules per sphere:	$N_W = V_S/v_W$
3 Number of water molecules that reside on the surface of each sphere:	$N^W_\sigma = S_S/a_W$
4 Total surface area of the sphere-necklace:	$\sum^T_S = S_S N_S$
5 Total surface energy:	$E^T_S = \gamma \sum^T_S$
6 Total number of water molecules in the sample:	$N^W_{Tot.} = N_W N_S$
7 Total number of water molecules on the surface:	$N^W{}_\Sigma = N^W_\sigma N_S$
8 Number of free water molecules:	$N^W_F = N^W_{Tot} - N^W{}_\Sigma$
b – Cylinder	
10 Total surface area:	$\sum^T_C = S_C N_S$ **
11 Total surface energy:	$E^T_C = \sum^T_C x\gamma$
12 Saved energy:	$\Delta E = E^T_S - E^T_C$

*V_T depends on the sample investigated. **There are as many elementary cylinders as spheres

val that is necessary to wait for observing them again is not always the same; it depends on several parameters that are difficult to control. The above findings confirm that the two processes investigated are indeed reproducible, but not reversible.

The energy balance

For each sample after the percolation transition the total energy released in the DSC freezing exotherms was measured.

The same procedure was applied to the corresponding melting endotherms, in the latter case the total heat absorbed upon the melting of the previously frozen sample was evaluated. Since freezing and melting processes are first order phase transitions, one would expect the heat released in the DSC-exo spectra to be equal to that absorbed in the DSC-endo ones. This was found to apply rigorously to the microemulsion state (Fig 1). However under the experimental conditions imposed to the system in the actual research, the above behavior was found not to apply. There is an energy difference ΔE(mJ) between the energy associated with the thermal events recorded upon melting the frozen samples and that associated with the thermal events obtained upon freezing the liquid ones. The ΔE difference was well above the experimental errors. The energy difference increases if the freezing spectra are measured after the bicontinuous transition.

The above result was interpreted as due to a difference arising because of a structural assessment of the sample. As a matter of fact, for instance, after the bicontinuous transition, we are freezing a different structure that is also energetically less expensive because it has a lower surface-to-volume ratio.

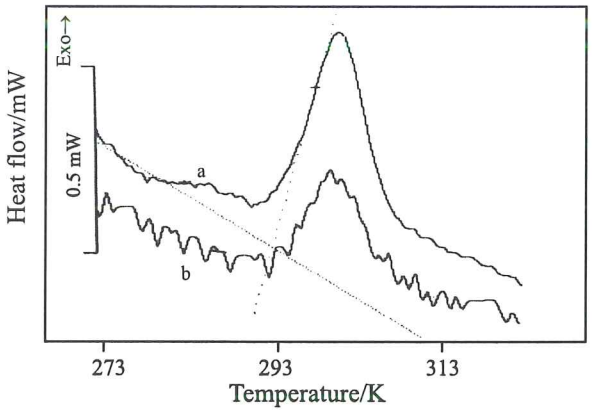

Fig. 5 The exothermal peak recorded as a function of increasing temperature of a sample taken for 30 min at 313 K and, thereafter processed for the measure of the percolative transition. Instead of the transition, the thermal event of exothermal nature was detected. Curve a – sample 7.67 mg; curve b – sample of 2.353 mg

The measured energy differences ΔE is reported in Table 5 for a few representative samples.

A very peculiar result is shown in Fig. 5: a thermal event of exothermal nature was recorded upon rising the temperature from 258 to 313 K. The exotherm occurs at 292.6 K (Onset Method).

We point out that the sample was taken for half an hour at 313 K. Therefore the sample temperature was lowered to 268 K and then measured again in the usual range (258–313) K for the detection of the percolation transition.

Through trials and errors we finally succeeded in reproducing the above described exotherm on other samples too.

Table 5 Energy balance

Sample/mg	ΔE_{Model}/mJ	$^{*}\Delta E_{DSC1}$/mJ	$^{*}\Delta E_{DSC2}$/mJ	**Exotherm/mJ
2.353	6.87	7.00		6.66
5.051	14.72	12.83	34.40	
5.225	15.20		52.14	
7.670	22.42	29.22		22.31

$^{*}\Delta E_{DSC1}$ – measured after the percolation transition; ΔE_{DSC2} – measured after the bicontinuous transition. **Exotherm: energy released by the exothermal peak (Fig. 5)

Table 6 Free and interfacial water molecules: comparison between the model and the DSC analysis

Sample/mg	Total H_2O molecules (10^{19})	Free H_2O molecules (10^{19})	*Interfacial H_2O molecules (10^{19})	Analysis type
2.353	2.900	2.314	0.586	DSC
	2.890	2.370	0.520	Model
5.051	6.207	4.946	1.261	DSC
	6.187	5.073	1.114	Model
5.225	6.410	4.899	1.511	DSC
	6.389	5.239	1.150	Model
7.67	9.453	7.277	2.176	DSC
	9.435	7.737	1.698	Model

*Interfacial: read 'Not Free water' for the DSC data and 'Surface water' for the model

Again the result was ascribed to an amount of energy saved because of an assessment of the system toward a less expensive structure.

This time however the sample, being taken at a fixed temperature, may have changed its structure and 'stocked' the surplus energy without having the possibility of getting rid of it. As soon as the new measure had started, instead of going through the percolation transition, evidently already accomplished, the saved amount of energy was released in the form of an exothermal peak.

The purpose of the model described in the previous section, was that of verifying the order of magnitude of the energy change associated with a decrease of the 'geometrical surface' of a system because of a transition from a water-sphere-necklace to a water cylindrical channel with the same volume of water and the same length of the necklace.

The results obtained are given in Table 5 where all the data of the energy balance analysis are reported in order to facilitate a parallel comparison between the results gathered with the model and the DSC measures.

The number of water molecules, (Table 4, points 6–8), labelled as 'free' (N_F^W), i.e. not on the sphere-surfaces, as well as the number of water molecules that reside on the sphere-surfaces (N_Σ^W), estimated with the model, are given in Table 6 where also those evaluated by means of the DSC analysis are reported. The two groups of data are distinguished by the entry 'DSC' and 'Model'. Looking upon Table 6 it emerges that the estimate of the amount of surface water resulting from the model, is always lower than the corresponding 'not-free –water' fraction obtained by DSC analysis. As a consequence, the DSC 'free-water' fraction is less than that estimated with the model.

It should be noted that in the DSC case, the not-free water includes the water bound to the hydrophilic groups of the AOT surfactant as well as that 'trapped' within the AOT inverse micelles dispersed in the decane phase. Several authors report that in the AOT inverse micelle the water is definitely in the bound state [1–5]. From the c.m.c. (critical micellar concentration) of AOT in decane, 0.73 mM [14], knowing the mass of the different components used to formulate the sample, it is possible to evaluate the percent of AOT involved in the formation of the inverse micelle in the oil as well as that devoted to stabilize the microemulsion droplets. The result shows that the 18% of the AOT is utilized to stabilize the water-oil interphase of the droplets while, up to the 82% is in the inverse micellar state. A careful investigation about the role of the surfactant-water interaction in driving the surfactants solubility, the self-association processes as well as the partitioning of water as 'free', 'interfacial' and 'bound', is reported in [15]. The DSC analysis confirms that the 'not-free-water' fraction, for the system investigated, ranges between the 24–28%. The model although very simple and schematic, has given results that are consistent with the hypotheses formulated and has helped evidencing the energy saved because of a structural change towards a lower surface-to-volume ratio.

Last but not least it is worthwhile to underline that the temperature at which the exothermal peak of Fig. 5 occurs, upon rising the temperature is the same at which the percolation transition was detected for the given sample: 292.6 K.

Acknowledgements

This work was supported by the Italian MUR, PRIN2005 and INFM.

References

1 J. S. Huang, J. Surface Sci. Technol., 5 (1989) 83
2 S. H. Chen, Ann. Rev. Phys. Chem., 37 (1986) 351.
3 S. J. Chen, D. F. Evans, B. W. Ninham, D. J. Mitchell, F. D. Blum and S. Pickup, J. Phys. Chem., 90 (1986) 842.
4 J. Israelachvili, Physics of Amphiphiles: Micelles, Vesicles and Microemulsions, V. De Giorgio and M. Corti Eds, Course XC, Proc. Int. School Phys. Enrico Fermi, Italian Physical Soc., North Holland, Amsterdam, 1985, p. 24.
5 J. Rouch, N. M. Ziou, C. Cametti, P. Codastefano, P. Tartaglia and S. H. Chen, J. Phys.: Condens. Matter, 2 (1990) SA353-SA357.
6 D. Senatra, Thermal Behavior of Dispersed Systems, N. Garti Ed., Marcel Dekker, Inc. New York, Basel 2000, p. 203.
7 D. Vollmer, J. Vollmer and H. F. Heike, Europhys. Lett., 26 (1994) 389.
8 P. L. Luisi, P. Meier, V. Imre and A. Pande, Reverse Micelles, P. L. Luisi and B. Straub, Eds, Plenum Publ. 1984.
9 L. Letamendia, E. Pru-Lestret, P. Panizza, J. Rouch, F. Sciortino, P. Tartaglia, C. Hashimoto, H. Ushiki and D. Risso, Physica A, 300 (2001) 53.
10 D. Senatra, R. Pratesi and L. Pieraccini, J. Thermal Anal., 51 (1998) 79.
11 D. Senatra, C. M. C. Gambi, M. Carlà and A. Chittofrati, J. Therm. Anal. Cal., 56 (1999) 1335.
12 D. Senatra, Z. Zhou and L. Pieraccini, Progr. Colloid Polymer. Sci., 73 (1987) 66.
13 P. C. Hiemenz, Principles of Colloid and Surface Chemistry, J. J. Lagowski Ed., 1977, p.1, Marcel Dekker Inc., New York- Basel.
14 K. M. Kotlarchyk, J. S. Huang and S. H. Chen, J. Phys. Chem., 89 (1985) 4382.
15 M. Fernandez-Tarrio, C. Alvarez-Lorenzo and A. Concheiro, J. Therm. Anal, Cal., 87 (2007) 171.

Received: June 28, 2007
Accepted: October 18, 2007

DOI: 10.1007/s10973-007-8611-9